

Woody-to-total area ratio determination with a multispectral canopy imager

JIE ZOU,¹ GUANGJIAN YAN,^{1,2,*} LING ZHU¹ and WUMING ZHANG¹

¹ School of Geography, State Key Laboratory of Remote Sensing Science, Jointly Sponsored by Beijing Normal University and the Institute of Remote Sensing Applications of Chinese Academy of Sciences, Beijing Normal University, China

² Corresponding author (gjyan@bnu.edu.cn)

Received December 4, 2008; accepted May 17, 2009; published online June 24, 2009

Summary Leaf area index (LAI) – defined as one half of the total green leaf area per unit ground surface area – can be determined by direct or indirect methods. Three major sources of errors exist in indirect LAI measurements: within-shoot clumping, beyond-shoot clumping and non-photosynthetic components. The effect of non-photosynthetic components on LAI measurements can be described by the woody-to-total area ratio, α ; however, no convenient and efficient indirect methods have been developed to estimate α , especially the variations in α with zenith angle θ , $\alpha(\theta)$. We describe the development and use of a multispectral canopy imager (MCI) to estimate α and $\alpha(\theta)$ by considering the effects of non-random distributions of canopy elements and woody components and the overestimation of needle-to-shoot area ratio on woody components. The MCI, which mainly comprises a near-infrared band camera (Fujifilm IS-1), two visible band cameras (Canon 40D), filters and a pan tilt, was developed to measure clumping index, woody-to-total area ratio and geometric parameters of isolated trees. Two typical sampling plots (Plots 1 and 5) chosen from among 16 permanent forest experiment plots were selected for the estimation of α and $\alpha(\theta)$. The non-random distributions of canopy elements and woody components were estimated separately at eight zenith angles (from 0° to 70° in increments of 10°) using MCI images based on the gap size distribution theory. The visible/near-infrared image pairs captured by the MCI were able to discriminate among sky, leaves, cloud and woody components. Based on three methods of estimation, we obtained woody-to-total area ratios of 0.24, 0.19, 0.19 for Plot 1 and 0.23, 0.18, 0.17 for Plot 5. If clumping effects were ignored, α values were overestimated by as much as 21% and 24% at Plots 1 and 5, respectively. We demonstrated that $\alpha(\theta)$ varied with the zenith angle, with variations in the range of 3–33% at Plot 1 and 2–65% at Plot 5. A new formula for the precise determination of LAI is proposed.

Keywords: clumping index, leaf area index, near-infrared photography, non-photosynthesis components, plant area index, woody area index, woody-to-total area ratio.

Introduction

Leaf area index (LAI), defined as one half of the total green leaf area per unit ground surface area (Chen and Black 1992), is an important parameter of canopy structure because it is related to many biophysical and physiological processes, including photosynthesis, respiration, transpiration, carbon cycling, net primary productivity and energy exchange. Therefore, LAI measurements are used in many fields, such as forestry, ecology, botany and agronomy (Ross 1981, Welles 1990).

Procedures for estimating LAI can be divided into direct and indirect methods. The direct method is time-consuming and labor-intensive and sometimes destructive to plants, so its use is generally limited and usually used to validate indirect methods. Compared with the direct method, indirect methods are quicker and more efficient, and they are usually based on optical methods that measure the canopy gap fraction as a function of the zenith angle. Typical indirect methods include LAI-2000 (LI-COR Corp., NE), HemiView (Delta-T Corp., Cambridge, UK) and TRAC (3rd Wave Engineering Corp., Ontario, Canada) (Jonckheere et al. 2004, Weiss et al. 2004). At present, there are three major sources of errors associated with indirect LAI measurements: within-shoot clumping, beyond-shoot clumping and the overestimation of non-photosynthetic components. Within-shoot clumping (needle-to-shoot area ratio, γ) can be measured using the geometric measurement method (Johnson 1984, Oker-Blom and Smolander 1988) or the volume displacement method (Beets 1977, Chen et al. 1997). TRAC and digital hemispherical photography (DHP) methods can be used to quantify the effects of beyond-shoot clumping. In contrast, there are no convenient and efficient indirect methods for measuring α , and especially the variations in α with zenith angle θ , $\alpha(\theta)$.

* Present address: School of Geography, Beijing Normal University, 19 Xijiekou Wai Street, Beijing, PRC.

The reason for the overestimation of non-photosynthetic components is that all components within canopies including woody components (e.g., stems, branches, flowers and fruits) contribute to intercepting beam radiation, and are included in the estimates of LAI based on optical methods. Therefore, optical methods provide an estimate of the plant area index (PAI; Neumann et al. 1989) or the vegetation area index (Fassnacht et al. 1994), rather than LAI. However, studies on the biophysical and physiological processes of forest canopies require a measure of LAI rather than a composite value of both leafy and woody areas because LAI determines the contribution of leaves to photosynthesis and ultimately dominates the exchange of heat, water and carbon in a forest. Therefore, it is essential to exclude the effects of woody components from LAI measurements, especially for applications that require precise LAI values.

Methods for measuring the woody area index (WAI) and the woody-to-total area ratio ($\alpha = \text{WAI}/\text{PAI}$) can also be classified into direct methods, which rely on destructive sampling and indirect methods, which are based on radiation sensors and photography. Direct destructive sampling methods usually involve measuring the woody area of representative trees within forest stands, similar to the procedure used for direct measurements of leaf area. The direct method has rarely been used to estimate α because of the huge investment in labor and time. Indirect optical methods usually involve taking measurements during both the leafless and leafy periods (e.g., using an LAI-2000 or by hemispherical photography). The values obtained during the leafless period are assumed to represent WAI for both the leafless and leafy periods, and differences in the contributions of small branches that are preferentially shaded by leaves during the leafy period are ignored. There are no leafless periods in evergreen forest stands, so these methods cannot be used in such forest stands. Another indirect method involves the use of a multiband vegetation imager (MVI; Kucharik et al. 1997, 1998a, 1998b). Because the MVI can make visible (VIS) and near-infrared (NIR) bands images, it can be used to quantify the effects of woody components on LAI measurements by discriminating between leaves, branches, stems, sky, etc.

The best procedure for deriving WAI remains controversial. If the entire canopy branch and stem areas were subtracted from the final PAI estimate (after correcting for canopy non-randomness), this is equivalent to assuming that small branches are not preferentially shaded by leaves or shoots but are randomly positioned in photosynthetically active foliage. However, if leaves or shoots preferentially mask small branches within the canopy, woody components may contribute much less to obscuring sky than their WAI because the location of woody components is correlated with leaf or shoot location in the crown. Thus, as for indirect photographic methods for estimating WAI, it is assumed that small branches are preferentially shaded by leaves or shoots. This assumption affects the gap fraction and the woody components clumping index, and hence

the WAI estimations. Small branches that are preferentially shaded by leaves or shoots within canopies will usually make the gap fraction (leaves or shoots and sky are regarded as gaps in WAI and woody components clumping index calculations) become larger; as a result, the effective WAI will be underestimated. Similarly, small branches preferentially shaded by leaves or shoots will enlarge some gap sizes that were used to estimate the woody components clumping index; therefore, the clumping index of woody components will be underestimated. Clumping effects of forest canopies are usually introduced by large gaps. Because shaded branches are generally small, their effect on estimates of the woody components clumping index should also be small compared with the effective WAI estimation. Therefore, the shade between woody components and leaves or shoots will introduce a certain degree of underestimation in the estimation of WAI.

Measurements of α have rarely been made. Published values of α range from 0.03 to 0.41. For instance, based on a destructive sampling method of seven boreal forest species at different growth stages and locations, Gower et al. (1999) concluded that the contributions of woody components to PAI range from 0.05 to 0.35. Deblonde et al. (1994) estimated α values of 0.08–0.12 and 0.10–0.33 for stands of *Pinus resinosa* Aiton and *Pinus banksiana* Lamb., respectively, using the direct method. Compared with the direct method, few studies based on indirect methods have measured α . Most indirect methods estimate α based on LAI-2000 measurements made during both the leafless and leafy periods. For example, Breda (2003) investigated 70 oak stands during the leafless and leafy periods within a year and found that α ranged from 0.07 to 0.40 and WAI ranged from 0.26 to 2.45. Barclay et al. (2000) estimated mean α values of 0.41, 0.41 and 0.25 for all trees in stands of *Pseudotsuga menziesii* (Mirb.) Franco, *Acer macrophyllum* Pursh. and *Alnus rubra* Bong., respectively, by a combination of LAI-2000 measurements and measurements of various parameters, such as stem location, diameter, height and height-to-live-crown. The MVI provides a method for measuring WAI and α , with WAI estimated as (Kucharik et al. 1997)

$$\begin{aligned} \text{WAI} &= B + \frac{1}{2}\xi S, \\ B &= B_e/\Omega_b(0) \text{ or } B = \frac{B_e^* + \varepsilon \text{LAI}}{\Omega_b(0)}, \end{aligned} \quad (1)$$

where B is the branch area index, B_e and B_e^* are the effective branch area indices during the leafless and leafy periods, respectively, ξ is a correction factor that accounts for the fraction of hemi-surface area that is projected in the view direction of the camera, S is the stem hemi-surface area from the ground to the base of live crown, $\Omega_b(0)$ is the clumping index at the zenith angle of 0° during the leafless period, LAI is the leaf area index derived from allometric equations and ε is an empirical correction factor for branch hemi-surface area that the MVI cannot

view in the canopy after leaf emergence based on pre-leaf emergence measurements of B . There are two difficulties associated with the use of MVI for determining WAI. First, reliable values of S and ξ are difficult to obtain; second, because of the limitations of the photographic method, it is difficult to make the MVI view only the whole canopy and the upper half of the stem of a single tree within a forest stand (Kucharik et al. 1998b). During a BOREAS project, MVI was used at four sites, and the results showed that the errors in MVI estimates were within 10–40% of the direct measurements. Although the results were not very good, it may be possible to develop a device based on some of the principles of the MVI that can measure WAI and α with much greater precision.

Because α is a dynamic parameter that varies with, for example, season, growth stage, location and defoliation, it should be estimated during every LAI measurement campaign. However, the direct method of measuring α is inefficient, so a new indirect method is needed that can measure α quickly and easily. Up to now, there is no information on the variation in α with zenith angles and it is generally assumed that α is constant at all zenith angles. In addition, the spatial distribution of woody components has been assumed to be random. The assumption of randomness can result in large errors that exceed 100% in some conifer forests (Fassnacht et al. 1994). Thus, it is necessary to account for the non-random distribution of woody components during α and WAI measurements. In this study, a new device, a multispectral canopy imager (MCI), was used to determine the woody-to-total area ratio. The MCI can be used for rapid and high-frequency measurements of α , by considering within-shoot and beyond-shoot clumping effects of canopy elements and woody components. We also studied the variation in $\alpha(\theta)$.

Theory

Effective PAI and WAI

The effective PAI and WAI are calculated without considering clumping effects, and their values at zenith angle θ can be estimated as

$$\text{PAI}_e(\theta) = \frac{-\ln[p(\theta)] \cos(\theta)}{G(\theta)} \quad (2)$$

and

$$\text{WAI}_e(\theta) = \frac{-\ln[p_w(\theta)] \cos(\theta)}{G(\theta)}, \quad (3)$$

where $\text{PAI}_e(\theta)$ is the effective PAI at zenith angle θ , $\text{WAI}_e(\theta)$ is the effective WAI at zenith angle θ , $p(\theta)$ is the measured canopy gap fraction at zenith angle θ , $p_w(\theta)$ is the measured woody components gap fraction (leafy components and sky are regarded as woody components gap fraction in WAI and woody components

clumping index estimations) at zenith angle θ and $G(\theta)$ is the projection coefficient characterizing the foliage angle distribution.

Optical methods are often used to measure the canopy gap fraction based on radiation transmittance through the canopy. Assuming a random spatial distribution of leaves or shoots and woody components, the effective PAI and WAI can be accurately estimated based on the Miller theory (Miller 1967)

$$\text{PAI}_e = -2 \int_0^{\pi/2} \ln[p(\theta)] \cos(\theta) \sin(\theta) d\theta \quad (4)$$

and

$$\text{WAI}_e = -2 \int_0^{\pi/2} \ln[p_w(\theta)] \cos(\theta) \sin(\theta) d\theta, \quad (5)$$

where $p(\theta)$ and $p_w(\theta)$ are averaged over the entire azimuthal angle range.

In our study, the zenith angles used for the determination of α ranged from 0° to 75° , which is similar to the 148° field of view (FOV) of the LAI-2000. The estimated woody-to-total area ratios can be used to correct the PAI_e measured by the LAI-2000. To maintain consistency with the LAI-2000 measurements, the calculations of PAI_e and WAI_e , which were used to estimate α , were similar to the calculations developed for the LAI-2000. Equations (4) and (5) were integrated by summing the products of PAI_{ei} ($-\ln[p(\theta_i)]\cos(\theta_i)$), WAI_{ei} ($-\ln[p_w(\theta_i)]\cos(\theta_i)$) and W_i ($\sin(\theta_i)d\theta_i$) as

$$\text{PAI}_e = 2 \sum_{i=1}^8 \text{PAI}_{ei} W_i \quad (6)$$

and

$$\text{WAI}_e = 2 \sum_{i=1}^8 \text{WAI}_{ei} W_i. \quad (7)$$

The values of W_i were computed by dividing the interval from 0° to 90° into eight uneven intervals. When normalized to 1.0, values of W_i are 0.0038, 0.0303, 0.0596, 0.0872, 0.1120, 0.1335, 0.1510 and 0.4226 corresponding to center zenith angles of 0, 10, 20, 30, 40, 50, 60 and 70° , respectively (Li-Cor 1989).

PAI, WAI and LAI

PAI and WAI calculations Values of PAI and WAI at zenith angle θ can be estimated based on the following equations by correcting for clumping effects

$$\text{PAI}(\theta) = \text{PAI}_e(\theta) \cdot \gamma_e(\theta) / \Omega_e(\theta) \quad (8)$$

and

$$\text{WAI}(\theta) = \text{WAI}_e(\theta) / \Omega_w(\theta), \quad (9)$$

where $\text{PAI}(\theta)$ is the plant area index at zenith angle θ , $\text{WAI}(\theta)$ is the woody area index at zenith angle θ , $\gamma_e(\theta)$

is the needle-to-shoot area ratio at zenith angle θ , $\Omega_c(\theta)$ is the canopy elements clumping index of zenith angle θ at scales larger than the shoot and $\Omega_w(\theta)$ is the woody components clumping index at zenith angle θ . For WAI estimation, there are no within-shoot clumping effects and $\gamma_e(\theta) = 1$.

Similar to Eqs. (8) and (9), PAI and WAI can be estimated as

$$\text{PAI} = \text{PAI}_e \cdot \gamma_e / \Omega_e \quad (10)$$

and

$$\text{WAI} = \text{WAI}_e / \Omega_w, \quad (11)$$

where γ_e is the needle-to-shoot area ratio, Ω_e is the canopy elements clumping index and Ω_w is the woody components clumping index. Further, PAI_{30-60} and WAI_{30-60} can be calculated as

$$\text{PAI}_{30-60} = \text{PAI}_e \cdot \gamma_e / \Omega_{e(30-60)} \quad (12)$$

and

$$\text{WAI}_{30-60} = \text{WAI}_e / \Omega_{w(30-60)}, \quad (13)$$

where $\Omega_{e(30-60)}$ is the mean canopy elements clumping index at zenith angle ranging from 30° to 60° and $\Omega_{w(30-60)}$ is the mean woody components clumping index at zenith angle ranging from 30° to 60° .

LAI calculation Because optical methods can only measure PAI_e , a formula developed by Chen et al. (1997) was used to convert PAI_e to LAI:

$$\text{LAI} = (1 - \alpha) \cdot \text{PAI}_e \cdot \gamma / \Omega_e. \quad (14)$$

Because $\Omega_e(\theta)$, $\gamma_e(\theta)$ and $\alpha(\theta)$ are not constant at all zenith angles, a formula for directional LAI determination is proposed:

$$\text{LAI}(\theta) = [1 - \alpha(\theta)] \cdot \text{PAI}_e(\theta) \cdot \gamma_e(\theta) / \Omega_e(\theta), \quad (15)$$

where $\text{LAI}(\theta)$ is the leaf area index at zenith angle θ and $\alpha(\theta)$ is the woody-to-total area ratio at zenith angle θ .

Clumping index

Foliage clumping (Nilson 1971) is separated into within-shoot clumping and beyond-shoot clumping (Chen and Cihlar 1995a). This separation is necessary because optical methods are generally incapable of measuring the gaps between needles within a shoot. The clumping index $\Omega(\theta)$ can be separated into two components as

$$\Omega(\theta) = \frac{\Omega_e(\theta)}{\gamma_e}, \quad (16)$$

where γ_e is the needle-to-shoot area ratio quantifying the effect of foliage clumping within a shoot (it increases with increasing clumping) and $\Omega_e(\theta)$ includes the effect of

canopy elements (including leafy and woody components) clumping at scales larger than the shoot (it decreases with increasing clumping) (Chen 1996).

Within-shoot clumping Branches and stems were considered as foliage elements and the value of the needle-to-shoot area ratio was assumed to be 1 in LAI measurements. But as described by Eq. (14), γ (> 1) would correct the WAI_e of the woody components, which was included in PAI_e ; therefore, it will introduce an overestimation of LAI. To correct for the overestimation of γ for woody components, $\gamma_e(\theta)$ for leafy and woody components at the zenith angle of θ was estimated as

$$\gamma_e(\theta) = 1 \times \text{WAI}(\theta) / \text{PAI}(\theta) + \gamma \times [\text{PAI}(\theta) - \text{WAI}(\theta)] / \text{PAI}(\theta), \quad (17)$$

where $\gamma_e(\theta)$ is the needle-to-shoot area ratio for all leafy and woody components, γ is the effective needle-to-shoot area ratio, which can be measured directly. The principle of the correction is based on the proportion of WAI included in PAI. The final needle-to-shoot area ratio for the whole plot can be estimated as

$$\gamma_e = 1 \times \text{WAI} / \text{PAI} + \gamma \times [\text{PAI} - \text{WAI}] / \text{PAI}. \quad (18)$$

Beyond-shoot clumping Two classic approaches can be used to quantify the beyond-shoot clumping effects: finite-length averaging and gap size distribution methods. The finite-length averaging method calculates the mean gap fraction within each finite length; the finite length equals 10 times the mean width of a foliage element. It is assumed that the foliage within the finite length is random and the segment contains gaps (Lang and Xiang 1986). However, because the foliage within the finite length is not randomly distributed and some segments may not contain any gaps, this assumption will introduce errors in the clumping index estimation. Furthermore, the finite-length averaging method provides a measure that is equivalent to the clumping index between finite lengths. Therefore, we chose the gap size distribution method to determine the beyond-shoot clumping index estimation in this study.

Beyond-shoot clumping for canopy elements and woody components was quantified separately based on the gap size distribution theory as

$$\Omega_e(\theta) = \frac{\ln(F_m(0, \theta))}{\ln(F_{mr}(0, \theta))} \cdot \left[1 + \frac{F_m(0, \theta) - F_{mr}(0, \theta)}{1 - F_m(0, \theta)} \right] \quad (19)$$

and

$$\Omega_w(\theta) = \frac{\ln(F_{mw}(0, \theta))}{\ln(F_{mrw}(0, \theta))} \cdot \left[1 + \frac{F_{mw}(0, \theta) - F_{mrw}(0, \theta)}{1 - F_{mw}(0, \theta)} \right], \quad (20)$$

where $F_m(0, \theta)$ is the measured total canopy gap fraction at zenith angle θ (i.e., the accumulated gap fraction from the largest to the smallest gaps), $F_{mr}(0, \theta)$ is the total gap fraction after removing large gaps resulting from the non-random canopy elements distributions due to canopy structures such as tree crowns and branches (Chen and Cihlar 1995a, 1995b, Leblanc et al. 2002), $F_{mw}(0, \theta)$ is the measured total woody components gap fraction at zenith angle θ (i.e., the accumulated woody components gap fraction from the largest to the smallest gaps) and $F_{mrw}(0, \theta)$ is the total gap fraction after removing large gaps resulting from the non-random woody components distributions due to stems and branches.

Simulations of Five-Scale model show that the mean clumping index between 30° and 60° approximates the mean clumping index of all angles (Leblanc and Chen 2001). Therefore, the mean clumping indices of canopy elements ($\Omega_{c(30-60)}$) and woody components ($\Omega_{w(30-60)}$) were calculated based on Eqs. (19) and (20) by using the corresponding gap size distribution data sampled from zenith angles between 30° and 60°.

After LAI and WAI of the plots were estimated, the clumping indices of canopy elements and woody components for the two plots were calculated as

$$\Omega_c = (\text{PAI}_c \cdot \gamma_c) / \text{PAI} \quad (21)$$

and

$$\Omega_w = \text{WAI}_c / \text{WAI}. \quad (22)$$

Comparisons between the mean and final clumping indices were used to assess the robustness of the mean clumping indices used in Eqs. (12) and (13) for LAI measurements.

Woody-to-total area ratio

Generally, the effect of woody components on LAI measurements can be quantified by the woody-to-total area ratio, α . The effective woody-to-total area ratio and woody-to-total area ratio of each zenith angle can be determined as

$$\alpha_c(\theta) = \text{WAI}_c(\theta) / \text{PAI}_c(\theta) \quad (23)$$

and

$$\alpha(\theta) = \text{WAI}(\theta) / \text{PAI}(\theta), \quad (24)$$

where $\alpha_c(\theta)$ is the effective woody-to-total area ratio at zenith angle θ and $\alpha(\theta)$ is the woody-to-total area ratio at zenith angle θ . Similarly, with the values of WAI, WAI_c , PAI and PAI_c , the woody-to-total area ratio and effective woody-to-total area ratio can be estimated as

$$\alpha = \text{WAI} / \text{PAI} \quad (25)$$

and

$$\alpha_c = \text{WAI}_c / \text{PAI}_c, \quad (26)$$

where α is the woody-to-total area ratio and α_c is the effective woody-to-total area ratio. An estimate of α_{30-60} can be obtained by substituting WAI_{30-60} and PAI_{30-60} in Eq. (25).

Materials and methods

Site descriptions

Study sites are located at the middle reaches of the Heihe River area in a ~ 130-year-old natural coniferous forest that is on the north side of the Qilian Mountain, Gansu Province of China. An experimental plot of 100 × 100 m dominated by *Picea crassifolia* Kom. was selected on a relatively flat terrain. The experimental plot was divided into 16 sub-plots (hereafter Plots 1–16) each of 25 × 25 m. All of the plots were measured by five methods – LAI-2000, TRAC, HemiView, fisheye photography and MCI. The MCI was used to measure the LAI of *P. crassifolia* in a simultaneous airborne, satellite-borne and ground-based remote sensing field campaign in June 2008. To obtain precise LAI measurements, the MCI was also used to collect woody-to-total area ratio and clumping index data, which were then used to correct the measurements estimated by other indirect methods.

MCI

Overall design The MCI was designed to be easy-to-use, affordable and multipurpose. It was developed mainly: (1) to determine the woody-to-total area ratio and analyze its variation with zenith angles; (2) to derive the clumping index and analyze its variation with zenith and horizontal angles; and (3) to measure the geometric parameters, LAI and PAI of isolated trees, and to estimate the vertical distributions of LAI and PAI. The MCI captures VIS and NIR image pairs by exchanging the filters manually. For the MVI, the ratio of sunlit foliage radiances in the NIR to the VIS is 4:1, whereas for shaded foliage the ratio is about 2:1, and for branches, clouds and sky the ratio is about 1:1 (Kucharik et al. 1997). The wave bands of MCI are similar to those of MVI and, like those of the MVI, it has the ability to discriminate among leaves, sky, branches, stems, etc., based on co-registered NIR and VIS images. The fractions of sky, leaves and woody components of the classified images are extracted separately, and the effective PAI and WAI computed based on the gap fraction theory. Similar to TRAC and MVI methods, clumping indices are inferred from the classified images based on the gap size distribution theory (Chen 1996, Chen et al. 1997, Kucharik et al. 1997). Estimates of WAI, woody-to-total area ratio and clumping index at all zenith angles are facilitated using a pan tilt in the MCI that can arbitrarily revolve in the zenithal and horizontal directions. As for the measurements of isolated trees, to minimize the difficulties in the registration of image pairs captured from the three cameras, a synchronous



Figure 1. Illustration of the MCI. This figure appears in color in the online version of *Tree Physiology*.

exposure device was used to synchronize the exposure of the three cameras. Calculation of the three-dimensional measurements was based on a close-range photogrammetry method.

System hardware As shown in Figure 1, the MCI consists of the following components: (1) A near-infrared camera IS-1 (Fujifilm Corp., Tokyo, Japan) with the ability to image in the range of 400–900 nm. It can capture images corresponding to 3488×2616 pixels. The focal length ranges from 6.2 to 66.7 mm. (2) Two Canon 40D DSLR cameras coupled with two Canon EF f/2.8 USM 20 mm lenses. They have a maximum pixel capacity of about 10 megapixels. These two cameras are used only in single tree measurement. (3) A Velbon PH285 pan tilt (Velbon Corp., Tokyo, Japan) that carries the cameras and controls the rotation freely. (4) A surveying tripod (Leica Corp., Heerbrugg, Switzerland). (5) Three filters for the IS-1, including one VIS band-pass filter (F-Pro BW 58 mm UV-IR cut 486, made in Germany, 390–690 nm) and two NIR band-pass filters (Nature HL-OPTICS 760 nm, Nature HL-OPTICS 850 nm, made in China). (6) Three customized metallic equipments, including one aluminous arm about 1.2 m long and two aluminous links used to link the arm, the pan tilt and the tripod. (7) A synchronous exposure device and three camera plates. To obtain a maximum FOV, the focal length of IS-1 is usually fixed at 6.2 mm during image collection.

Data acquisitions A representative location in each of Plots 1 and 5 was chosen for α measurements in June 2008. Forest inventory was carried out for the entire site during the period of LAI measurements. The slope at Plots 1 and 5 was about 10° . Mean canopy heights at Plots 1 and 5 were 7.98 and 8.21 m, respectively. Two shoots were sampled from each plot, with mean shoot element widths of 36.39 and 45.99 mm for Plots 1 and 5, respectively. In this

field campaign, the IS-1 camera, operating in automatic exposure mode, was used only for forest canopy imaging. Woody-to-total area ratio measurements were carried out in the zenith directions from 0° to 90° at intervals of 10° , and each zenith direction measurement comprised six horizontal direction measurements at intervals of 60° . The focal length was fixed at 6.2 mm during measurements and the corresponding FOV was about $65.65^\circ \times 51.64^\circ$. Because six azimuthal measurements corresponding to each zenith angle constitute a concentric ring in the horizontal direction, we were able to perform a full hemispherical sampling of the forest canopies with 60 image pairs (10 zenith directions, with six image pairs in each zenith direction). The sampling scheme was similar to that used by the LAI-2000 and hemispherical photography methods. Restricted by the narrow bandwidth of 50 nm only, the NIR filter (850 nm) was not used in α measurements. The biggest problem associated with the MCI measurements was the non-synchronous acquisition of the VIS and NIR images because the filters had to be removed and installed manually. Forest canopies were moved by wind during the time of filter exchange, which required 5–30 s depending on the operator. To minimize the effects of canopy movement on each image pair, MCI measurements were made under windless or breezy conditions.

Image processing Because the images were not acquired simultaneously, the image pairs had to be co-registered. The center area of all images was clipped to 3188×533 pixels, representing an FOV of about $60^\circ \times 10^\circ$ in the horizontal and zenithal directions, respectively. First, images collected at zenith angles of 80° and 90° were discarded because terrain was included in the images. Each image was subdivided into four sub-images to minimize the effects of charge-coupled device gain and misclassification. Because of the low similarity between the VIS and NIR images within each image pair, the efficiency of feature-based automatic registration was low, even though the automatic registration method has been applied successfully in aspen and poplar forest stands for MVI. More algorithms need to be tested to find an appropriate automatic algorithm for robust registration between VIS and NIR bands images of coniferous forests. All image pairs were registered manually. Second, image pairs were classified based on the ISODATA unsupervised classification method. This method calculates class means evenly distributed in the data space, and then iteratively clusters the remaining pixels based on minimum distance techniques; therefore, it can make good use of the special spectral characteristics in the VIS and NIR bands for forest canopies. The normalized difference vegetation index ($\text{NDVI} = (\text{NIR} - \text{VIS}) / (\text{NIR} + \text{VIS})$) image can be calculated based on the NIR and VIS images. Sometimes, an NDVI mask is needed to identify mixed pixels that may be misclassified by the ISODATA unsupervised classification method, such as those for very small branches, shaded leaves, sunlit branches (NDVI), etc. Finally, all image pairs

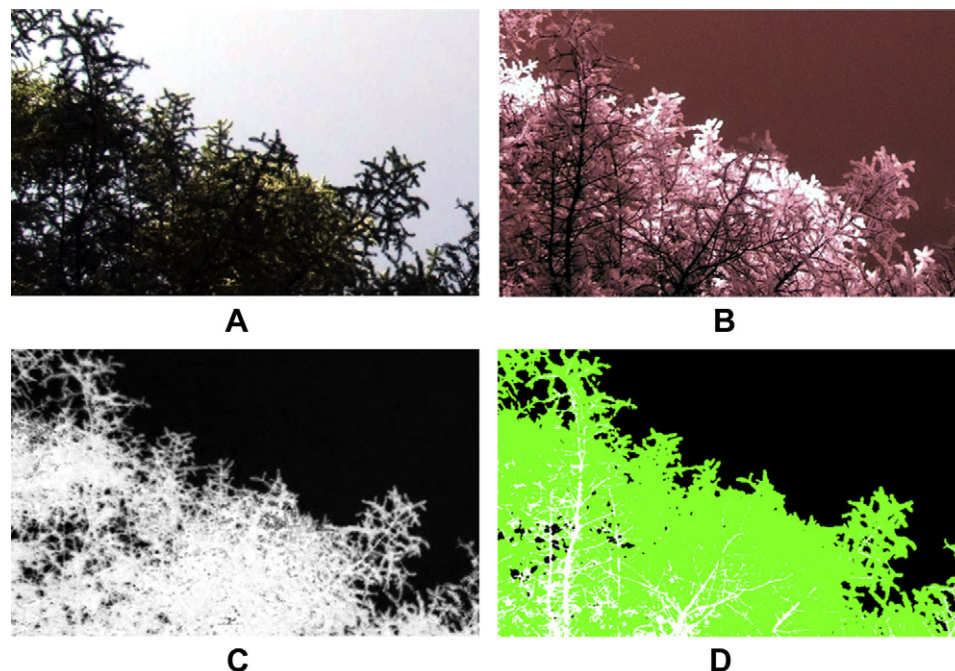


Figure 2. An image pair (VIS (A) and NIR (B)), the corresponding NDVI image (C) and the classified images (D). This figure appears in color in the online version of *Tree Physiology*.

were classified into three classes: leaves, woody components and sky (Figure 2).

Clumping index calculation

Because there are no simple methods to measure γ , we used a value of 1.3 measured in a spruce forest during a BOR-EAS campaign (Gower et al. 1999). After calculating $WAI_c(\theta)$, WAI_e , $PAI_c(\theta)$ and PAI_e , $\gamma_c(\theta)$ and γ_e can be estimated by Eqs. (17) and (18).

Canopy clumping indices of canopy elements and woody components were measured using the MCI. The key difference between TRAC and MCI is that the TRAC measures sun-fleck lengths, whereas the MCI views gap sizes within the canopy directly; therefore, it is insensitive to the position of the sun and the penumbra effect both of which affect the TRAC method. Compared with the TRAC resolution of 9.37 mm, MCI has a maximum resolution of 1.57 mm when the mean canopy height is about 8.21 m. The resolution of the MCI decreases with increasing zenith angle in the observation direction. The woody components include stems and branches, and their sizes vary greatly within forest canopies. Up to now, it has been difficult to make precise measurements of the mean woody element width. Mean shoot element width measured during the LAI measurements was used for the calculation of both canopy elements and woody components clumping indices. Gap size distribution data were sampled from the classified images by a combination of MVI and DHP methods (Kucharik et al. 1997, 1998a, 1998b, Leblanc et al. 2005). The sampling method of gap size distribution was similar to the DHP method that samples data from the centerline of corresponding zenith angle images. The full size of each pixel

was calculated as for the MVI method without assuming that 100 pixels represent a length of 1 m as in the DHP method. A minor difference between the MVI and MCI methods is that, in the latter method, the full size of each pixel increased with the zenith angle corresponding to each image. Two kinds of gap size distribution data were sampled from the center row of each image, one kind was sampled based on the rules that the sky components are regarded as gaps only for canopy elements clumping index calculation and the other was sampled based on the rules that the sky and leafy components are regarded as gaps and used for woody components clumping index estimation. Continuous gaps can be converted to gap lengths based on the size of each pixel.

The gap size distribution data at each zenith angle were sampled from the corresponding six azimuthal directions images, and the clumping indices for canopy elements ($\Omega_c(\theta)$) and woody components ($\Omega_w(\theta)$) were estimated based on the sampled gap size distribution data. The mean clumping indices of canopy elements ($\Omega_{c(30-60)}$) and woody components ($\Omega_{w(30-60)}$) between 30° and 60° (at intervals of 10°) were calculated based on all the images captured at these four zenith angles. After estimating LAI and WAI of the plot, the clumping indices of canopy elements and woody components can be calculated with Eqs. (21) and (22).

PAI, WAI and LAI estimation

Before calculating PAI and WAI, the statistical fractions of sky and woody components were estimated based on the classified images. The fractions of sky and woody components at each zenith angle are the mean statistical fractions of sky and woody components on the corresponding six

azimuthal classified images. Next, $\text{PAI}_c(\theta)$ and $\text{WAI}_c(\theta)$ at each zenith angle were estimated based on Eqs. (2) and (3) by assuming that $G(\theta) = 0.5$. After calculating the clumping index, we estimated $\text{PAI}(\theta)$ and $\text{WAI}(\theta)$, which consider the effects of within-shoot and beyond-shoot clumping, with Eqs. (8) and (9). Finally, the WAI and PAI of Plots 1 and 5 were calculated with Eqs. (10) and (11). The calculations of WAI and PAI differ from those for PAI_{30-60} and WAI_{30-60} in that $\Omega_{c(30-60)}$ and $\Omega_{w(30-60)}$ were used in the calculations of PAI_{30-60} and WAI_{30-60} .

Woody-to-total area ratio estimation

The $\alpha_c(\theta)$ and $\alpha(\theta)$ at each zenith angle were calculated with Eqs. (23) and (24), respectively. The difference between them is that $\alpha(\theta)$ was estimated by considering the clumping effects within $\text{WAI}_c(\theta)$ and $\text{PAI}_c(\theta)$. Three categories of woody-to-total area ratio for the whole plot were estimated, where α_c is the effective woody-to-total area ratio estimated with Eq. (26) and α is the woody-to-total area ratio estimated with Eq. (25) by considering the clumping effects within the WAI_c and PAI_c . Estimation of α_{30-60} is similar to that of α but based on WAI_{30-60} and PAI_{30-60} .

Results and discussion

Image processing analysis

The MCI cannot capture VIS and NIR images synchronously. Consequently, there was canopy movement in response to wind during the image pair collections. Although all images were taken under apparently windless conditions, a small portion of the upper shoots within a canopy was moving continually. Compared with the upper shoots in the canopy, other shoots in the canopy moved less. Because of the low similarity between shoots in the VIS and NIR images, the ground control points (GCPs) used for image pair co-registration were selected from the crossing points of branches; however, shoot movement cannot be completely eliminated by co-registration. Analysis of the co-registration errors for Plot 1 indicated that the total RMS errors were in the range of 0–2 pixels, and the GCP errors were in the range of 0–3 pixels.

A second source of error was associated with mixed pixels. Mixed pixels mostly occurred in three cases: fragmentary branches, moving shoots within the upper canopy, and sunlit stems and shaded shoots. The first case was caused by misclassification, and the third arose because sunlit stems and shaded shoots have similar digital number values in the image pairs. An analysis of the proportions of mixed pixels for woody components and sky at Plot 1 is shown in Figure 3. The proportion of mixed pixels for the woody components class was 12.79% at 0° zenith angle, and was introduced mainly by misclassification between sunlit stems and shaded leaves, and for fragmentary

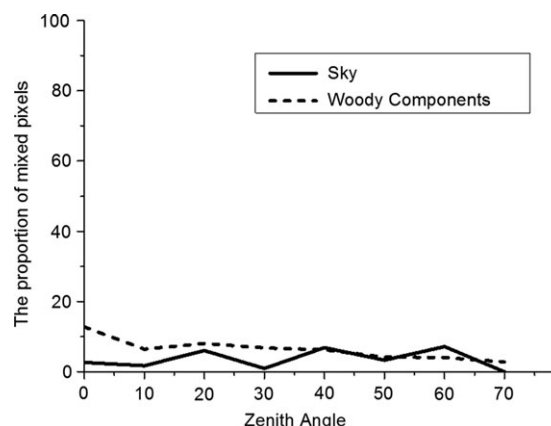


Figure 3. Proportion of mixed pixels for sky and woody components at Plot 1.

branches. For other zenith angles, the proportion of mixed pixels for woody components was usually between 3% and 8%. Compared with woody components, the sky is relatively homogeneous and the proportion of mixed pixels was usually between 0% and 7%. Errors introduced by mixed pixels on the estimates of WAI_c and PAI_c were about 0.04 and the proportions of errors for WAI_c and PAI_c were 6% and 1%, respectively.

Clumping index

The spatial arrangement of canopy elements and woody components in forest canopies usually follows a non-random distribution, thus deviating from the assumption of random distribution used to estimate LAI. To obtain precise LAI and WAI values for estimating α , corrections for the non-random distribution of canopy elements and woody components were required. Therefore, measurements of clumping index were a key step in our woody-to-total area ratio estimation. Figure 4 shows accumulated gap fraction profiles of canopy elements and woody components from Plot 1 at a zenith angle of 0°. Measured (F_m), reduced (F_{mr}) and theoretical random (F_r) curves were plotted against gap size (m). The largest gap sizes for canopy elements and woody components were 2.28 and 4.71 m, respectively (Figure 4). Even the largest gap size of canopy elements was smaller than that of the woody components; the proportion of reduced gap sizes for canopy elements was larger than that of the woody components. Furthermore, when calculating the clumping index, the number of iterations used to remove larger gaps within F_m was three for canopy elements, but only one for woody components. Both situations showed that canopy elements deviated more from the random distribution pattern than woody components. At Plot 1, the clumping indices of canopy elements and woody components at 0° zenith angle were 0.63 and 0.83, respectively. At both plots, the clumping indices of canopy elements and woody components at

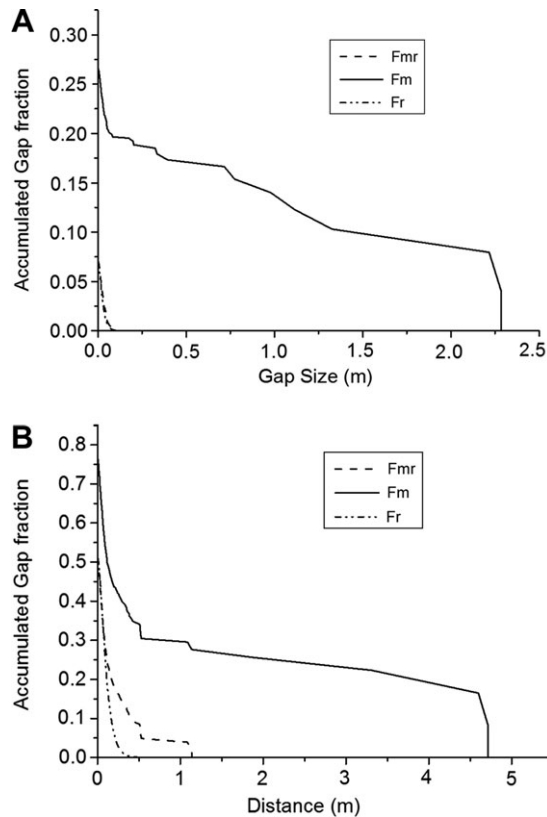


Figure 4. Measured (F_m), reduced (F_{mr}) and theoretical random (F_r) accumulated gap size distributions from Plot 1 at a zenith angle of 0° . (A) Canopy elements and (B) woody components.

zenith angles of 0° and 10° were smaller than at the other zenith angles (Figure 4), perhaps reflecting the high proportions of sky and the low proportions of branches in the images taken at small zenith angles, which will increase the degree of non-random distributions of the two components. For example, the fractions of sky and woody components at Plot 1 were 0.27 and 0.24, respectively, at 0° zenith angle, whereas the corresponding values at a zenith angle of 10° were 0.30 and 0.25. The clumping indices of canopy elements and woody components at 0° zenith angle for Plot 1 were similar to these values that range from 0.55 to 0.65, which were measured by the MVI method in the deciduous species aspen (Kucharik et al. 1997).

The effects of overestimating γ on calculations of woody components have not been examined previously, although

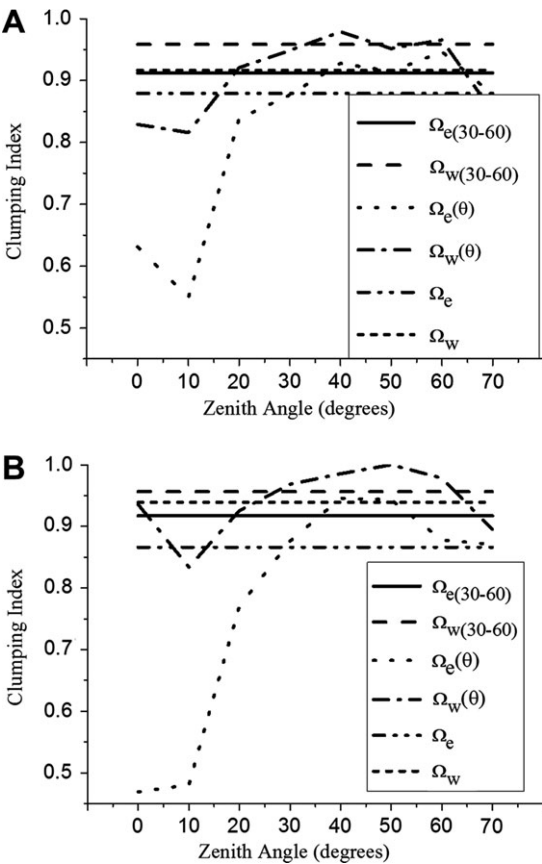


Figure 5. Clumping indices at Plot 1 (A) and Plot 5 (B).

such effects are existed to affect LAI values of coniferous forests. Traditional optical methods cannot remove the overestimation of γ because they are unable to discriminate between woody components and shoots. As can be inferred from Table 1, the difference between γ and γ_e was 6% at Plot 1 and 5% at Plot 5. Variations in $\gamma(\theta)$ at the eight zenith angles were small, mostly in the range of 0–2%, with a maximum of 3%, demonstrating that γ_e can substitute for $\gamma(\theta)$ at all zenith angles in LAI estimations.

Figure 5 shows that the curvilinear relationship between zenith angle and the canopy elements clumping index was similar at Plots 1 and 5, with peak values reached at zenith angles between 30° and 60° (Figure 5). The differences between $\Omega_{e(30-60)}$ and Ω_e , and between $\Omega_{w(30-60)}$ and Ω_w ranged from 2% to 6% in the two plots. The differences were

Table 1. Needle-to-shoot area ratio at Plots 1 and 5.

Zenith angle		0°	10°	20°	30°	40°	50°	60°	70°
Plot 1	$\gamma(\theta)$	1.24	1.23	1.23	1.21	1.21	1.22	1.23	1.24
	γ_e	1.23							
Plot 5	$\gamma(\theta)$	1.26	1.26	1.25	1.24	1.23	1.24	1.23	1.23
	γ_e	1.23							

small and so can usually be ignored in clumping index measurements. Comparisons among Ω_e and $\Omega_e(\theta)$, and among Ω_w and $\Omega_w(\theta)$ at zenith angles between 30° and 60° , revealed differences ranging from 0% to 9%, which were slightly larger than the difference between $\Omega_{e(30-60)}$ and Ω_e , and between $\Omega_{w(30-60)}$ and Ω_w . Variations in $\Omega_e(\theta)$ and $\Omega_w(\theta)$ at the eight zenith angles ranged from 0% to 38% at Plot 1 and from 0% to 46% at Plot 5. The data in Figure 5 indicate that the clumping index of woody components was always larger than the clumping index of elements, perhaps reflecting the presence of large amounts of small branches, especially at zenith angles between 40° and 60° .

WAI and PAI

At both plots, the sky fractions decreased with increasing zenith angle, whereas the woody fractions showed the opposite pattern. Within *P. crassifolia* forest stands, large amounts of dead branches accumulate in the lower canopies because most of the sunlight is intercepted by the upper canopies. Consideration of the extinction path correction indicated that $PAI_e(\theta)$ and $WAI_e(\theta)$ did not increase monotonously with increasing zenith angle. Figure 6 shows that $PAI_e(\theta)$ was usually underestimated compared with $PAI(\theta)$, because of the combined effects of within-shoot clumping and beyond-shoot clumping for canopy elements within the canopies. For Plots 1 and 5, $PAI_e(\theta)$ and $WAI_e(\theta)$ were usually 37–99% of the corresponding $PAI(\theta)$ and $WAI(\theta)$ and at the eight zenith angles. The largest variation was between $PAI_e(\theta)$ and $PAI(\theta)$ in Plot 5, where $PAI_e(\theta)$ was only 37% of $PAI(\theta)$. Compared with the large deviations between $PAI_e(\theta)$ and $PAI(\theta)$, the variations between $WAI_e(\theta)$ and $WAI(\theta)$ were relatively small, perhaps because of the larger clumping index of woody components and because there were no within-shoot clumping effects for woody components. The large deviations between $PAI_e(\theta)$ and $PAI(\theta)$, and the smaller deviations between $WAI_e(\theta)$ and $WAI(\theta)$ will result in errors in the estimation of α . Ideally, to derive a precise α value, foliage clumping indices for both canopy elements and woody components at all zenith angles should be considered when estimating α . In practice, because the variations of PAI and WAI values were within 2–6% of the PAI_{30-60} and WAI_{30-60} values (Figure 6), a mean clumping index for zenith angles from 30° to 60° can be substituted for the clumping indices at all zenith angles.

Woody-to-total area ratio

Table 2 summarizes all the parameters associated with the estimation of α . A plot of increasing zenith angle against $\alpha(\theta)$ yielded parabolic curves at Plots 1 and 5, where the minimum $\alpha(\theta)$ was at $\alpha(0)$ or $\alpha(10)$, and the maximum $\alpha(\theta)$ usually occurred at a zenith angle of 30° or 40° (Figure 7). At zenith angles of 30° and 40° , larger amounts of dead branches were located just below the live crowns than at the other zenith angles viewed by MCI. The differences

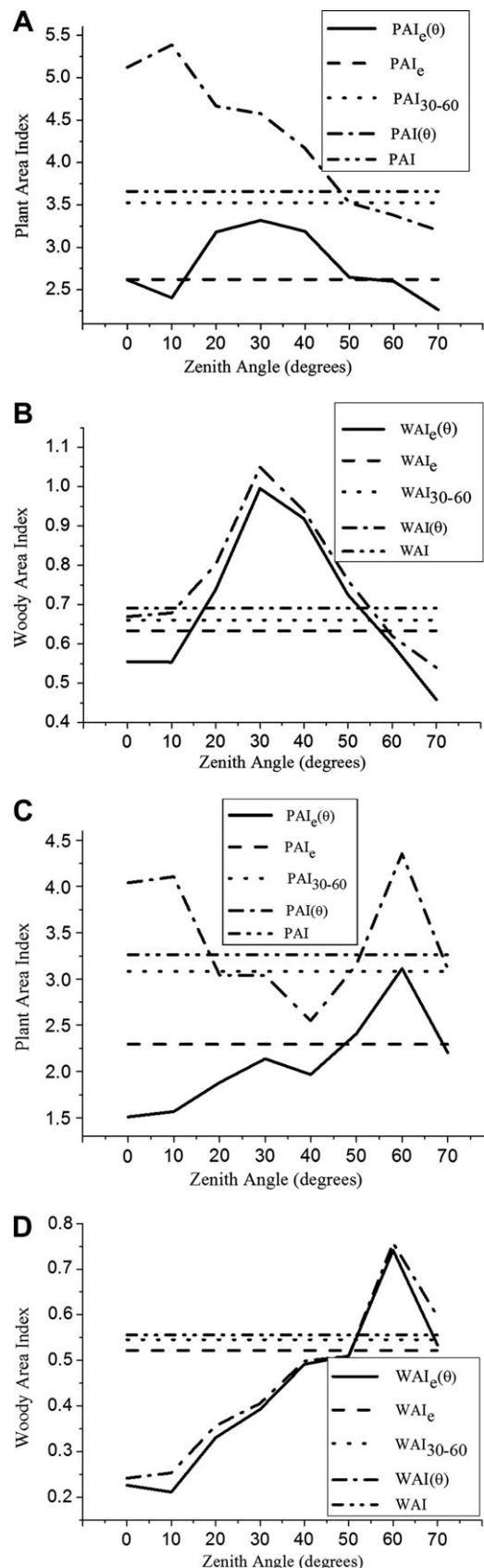


Figure 6. Values of PAI and WAI of Plot 1 (A and B) and Plot 5 (C and D).

Table 2. Summary of woody-to-total area ratio measurements.

	$\Omega_{e(30-60)}$	Ω_e	$\Omega_{w(30-60)}$	Ω_w	PAI _e	PAI ₃₀₋₆₀	PAI	WAI _e	WAI ₃₀₋₆₀	WAI	α_e	α_{30-60}	α
Plot 1	0.91	0.88	0.96	0.92	2.62	3.53	3.66	0.63	0.66	0.69	0.24	0.19	0.19
Plot 5	0.92	0.87	0.96	0.94	2.29	3.08	3.26	0.52	0.55	0.56	0.23	0.18	0.17

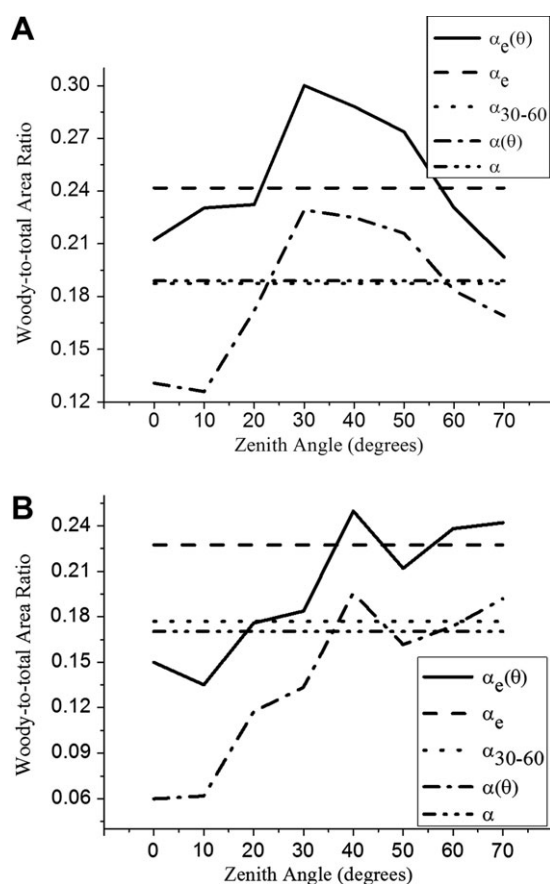


Figure 7. The woody-to-total area ratio of Plot 1 (A) and Plot 5 (B).

between α_e and α were 28% at Plot 1 and 25% at Plot 5. Because the effective woody-to-total area ratio (α_e) was estimated without correcting for the effects of within-shoot and beyond-shoot clumping, the large deviations between α_e and α clearly indicate that corrections for within-shoot and beyond-shoot clumping effects are critical for the precise estimation of α . Based on comparison with the $\alpha(\theta)$ values in Figure 7, $\alpha_e(\theta)$ was overestimated at all zenith angles. $\alpha(\theta)$ varied at the eight zenith angles measured with the variations falling in the range of 3–33% at Plot 1 and 2–65% at Plot 5. These variations demonstrate that the woody-to-total area ratio is not a constant at all zenith angles. However, optical methods have assumed that α is independent of the zenith angle and remove the woody components effects by using Eq. (14) which includes a constant at all zenith angles. Consequently, these methods may result in errors in the estimation of LAI. In contrast, after

we had estimated $\alpha(\theta)$, LAI(θ) values at the eight zenith angles were calculated with Eq. (15). Finally, LAI can be estimated by subtracting WAI from PAI also.

Although there are large differences between the sky fractions, woody fractions, PAI_e(θ), WAI_e(θ) and $\alpha_e(\theta)$ in the two plots, the difference between the two estimations of α was small, demonstrating that α is relatively stable within this natural forest stand.

In the direct method, canopies of single trees are sampled in the vertical direction, and the results are extrapolated from the sample trees to the whole site. The MCI method samples the canopies in hemispherical directions like other optical methods, such as the LAI-2000 and hemispherical photography. Therefore, α estimated from MCI measurements provides an opportunity to remove WAI, which is inherent in PAI_e measured by the optical methods, with the advantage of providing a consistent and sufficient sampling of the tree canopies. Because the LAI-2000 and hemispherical photography methods provide reliable PAI_e determinations when operated properly, a combination of the LAI-2000 or hemispherical photography method with MCI and TRAC is a good approach for ensuring accurate LAI determinations.

In conclusion, we developed an MCI that can capture image pairs of forest canopy in three different wavelength bands at arbitrary zenithal and horizontal directions. The MCI method can discriminate among sky, leaves, cloud and woody components. Because canopy elements and woody components usually behaved as non-random distributions and the degrees of deviation from randomness were more evident at small zenith angles, it is critical to correct for clumping effects on WAI_e(θ) and PAI_e(θ), which are used to estimate α . The effect of overestimation of γ on woody components was 6% at Plot 1 and 5% at Plot 5. These errors need to be considered when refining methods for determining LAI.

The woody-to-total area ratio was not a constant at all zenith angles. Variations in $\alpha(\theta)$ were in the range of 3–33% at Plot 1 and 2–65% at Plot 5. Differences between α_e and α were 28% at Plot 1 and 25% at Plot 5. Consequently, correcting for clumping effects is necessary when estimating α . Estimates of α at Plots 1 and 5 were 0.19 and 0.17, respectively. Future studies of LAI measurements should consider the variations in $\Omega_e(\theta)$, $\alpha_e(\theta)$ and $\gamma(\theta)$ at all zenith angles based on Eq. (15).

The MCI method samples the forest canopies in hemispherical directions like most of the indirect methods currently used. The woody-to-total area ratio measured by the MCI method is appropriate for correcting PAI_e

measured by other optical methods. Because the woody-to-total area ratio can be estimated quickly by the MCI method, it should be possible to develop the MCI method so that it can be used to measure the variations in α introduced by, for example, forest species, growth stage, location and defoliation.

Acknowledgments

This work was partially funded by NSFC (Grant No. 40871164), 973 Program (2007CB714402) and the European Commission (Call FP7-ENV-2007-1 Grant No. 212921) as part of the CEOP-AEGIS project (<http://www.ceop-aegis.org/>) coordinated by the Université de Strasbourg. The authors thank Ling Chen, Xinping Guo, Jing Li, Tianxing Wang and Dr. E. Chen for their help in the acquisition and processing of images. We also thank Prof. Jingming Chen of the University of Toronto for his useful suggestions on MCI. Two anonymous reviewers provided suggestions that improved the manuscript greatly. We would also like to thank Dr. Rozanne Poulson for her help in editing this manuscript.

References

- Barclay, H.J., J.A. Trofymow and R.I. Leach. 2000. Assessing bias from boles in calculating leaf area index in immature Douglas-fir with the LI-COR canopy analyzer. *Agric. For. Meteorol.* 100:255–260.
- Beets, P. 1977. Determination of the fascicle surface area for *Pinus radiata*. *N. Z. J. For. Sci.* 7:397–407.
- Breda, N.J.J. 2003. Ground-based measurements of leaf area index: a review of methods, instruments and current controversies. *J. Exp. Bot.* 54:2403–2417.
- Chen, J.M. 1996. Optically-based methods for measuring seasonal variation of leaf area index in boreal conifer stands. *Agric. For. Meteorol.* 80:135–163.
- Chen, J.M. and T.A. Black. 1992. Defining leaf area index for non-flat leaves. *Plant Cell Environ.* 15:421–429.
- Chen, J.M. and J. Cihlar. 1995a. Plant canopy gap-size analysis theory for improving optical measurements of leaf-area index. *Appl. Opt.* 34:6211–6222.
- Chen, J.M. and J. Cihlar. 1995b. Quantifying the effect of canopy architecture on optical measurements of leaf area index using two gap size analysis methods. *IEEE Trans. Geosci. Remote Sens.* 33:777–787.
- Chen, J.M., P.M. Rich, S.T. Gower, J.M. Norman and S. Plummer. 1997. Leaf area index of boreal forests: theory, techniques and measurements. *J. Geophys. Res.* 102:29429–29443.
- Deblonde, G., M. Penner and A. Royer. 1994. Measuring leaf area index with the Li-Cor LAI-2000 in pine stands. *Ecology* 75:1507–1511.
- Fassnacht, K.S., S.T. Gower, J.M. Norman and R.E. McMurtric. 1994. A comparison of optical and direct methods for estimating foliage surface area index in forests. *Agric. For. Meteorol.* 71:183–207.
- Gower, S.T., C.J. Kucharik and J.M. Norman. 1999. Direct and indirect estimation of leaf area index, fAPAR, and net primary production of terrestrial ecosystems. *Remote Sens. Environ.* 70:29–51.
- Johnson, J.D. 1984. A rapid technique for estimating total surface area of pine needles. *For. Sci.* 30:913–921.
- Jonckheere, I., S. Fleck, K. Nackaerts, B. Muys, P. Coppin, M. Weiss and F. Baret. 2004. Review of methods for in situ leaf area index determination: Part I. Theories, sensors and hemispherical photography. *Agric. For. Meteorol.* 121:19–35.
- Kucharik, C.J., J.M. Norman, L.M. Murdock and S.T. Gower. 1997. Characterizing canopy nonrandomness with a multi-band vegetation imager MVI. *J. Geophys. Res.* 102:455–473.
- Kucharik, C.J., J.M. Norman and S.T. Gower. 1998a. Measurements of leaf orientation, light distribution and sunlit leaf area in a boreal aspen forest. *Agric. For. Meteorol.* 91:127–148.
- Kucharik, C.J., J.M. Norman and S.T. Gower. 1998b. Measurements of branch area and adjusting leaf area index indirect measurements. *Agric. For. Meteorol.* 91:69–88.
- Lang, A.R.G. and Y. Xiang. 1986. Estimation of leaf area index from transmission of direct sunlight in discontinuous canopies. *Agric. For. Meteorol.* 37:229–243.
- Leblanc, S.G. and J.M. Chen. 2001. A practical scheme for correcting multiple scattering effects on optical LAI measurements. *Agric. For. Meteorol.* 110:125–139.
- Leblanc, S.G., J.M. Chen and M. Kwong. 2002. Tracing and radiation architecture of canopies TRAC manual version 2.1.3. 3rd Wave Engineering, Ontario, Canada.
- Leblanc, S.G., J.M. Chen, R. Fernandes, D.W. Deering and A. Conley. 2005. Methodology comparison for canopy structure parameters extraction from digital hemispherical photography in boreal forests. *Agric. For. Meteorol.* 129:187–207.
- Li-Cor. 1989. LAI-2000 plant canopy analyzer instruction manual. Licor Inc., NE.
- Miller, J.B. 1967. A formula for average foliage density. *Aust. J. Bot.* 15:141–144.
- Nilson, T. 1971. A theoretical analysis of the frequency of gaps in plant stands. *Agric. For. Meteorol.* 8:25–38.
- Neumann, H.H., G. Den Hartog and R.H. Shaw. 1989. Leaf area measurements based on hemispheric photographs and leaf-litter collection in a deciduous forest during autumn leaf-fall. *Agric. For. Meteorol.* 45:325–345.
- Oker-Blom, P. and H. Smolander. 1988. The ratio of shoot silhouette area to total needle area in Scots pine. *For. Sci.* 34:894–906.
- Ross, J. 1981. The radiation regime and architecture of plant stands. Dr. W. Junk Publ., The Hague.
- Weiss, M., F. Baret, G.J. Smith, I. Jonckheere and P. Coppin. 2004. Review of methods for in situ leaf area index (LAI) determination: Part II. Estimation of LAI, errors and sampling. *Agric. For. Meteorol.* 121:37–53.
- Welles, J.M. 1990. Some indirect methods of estimating canopy structure. *Remote Sens. Rev.* 5:31–43.